NEW INSIGHTS ON MODERN AGE COINS BY CALIBRATION-FREE LASER-INDUCED BREAKDOWN SPECTROSCOPY METHOD AND CHEMOMETRIC APPROACHES**

S. Awasthi [1], R. Kumar [2*], R. K. Pandey [3], A. Kumar Rai [4*]

[1] M. M. Mahila College at V. K. S. University, Ara, India
[2] C. M. P. College at University of Allahabad, Prayagraj, India; e-mail: rohit.02dec@gmail.com
[3] School of Engineering at University of Petroleum and Energy Studies, Energy Acres, Bidholi, Dehradun, India
[4] University of Allahabad, Prayagraj, India; e-mail: awadheshkrai@rediffmail.com

The elemental composition of one- and two-rupee coins issued in different years by the Reserve Bank of India (RBI) was investigated using laser-induced breakdown spectroscopy (LIBS). Aiming to preserve the surfaces of coins, the LIBS technique can perform real-time analysis of latent fingerprints of samples. The study is important as it has been observed that there are specific differences in the elemental compositions of coins that are not mentioned by the RBI. The study could also be used as a reference document for identifying and avoiding the circulation of counterfeit coins. Concentrations of constituents present in these coins have been determined by the calibration-free LIBS method. Furthermore, the current report employs appropriate statistical methods like principal component analysis and partial least square regression for the interpretation of complex data obtained from LIBS experiments, both qualitatively and quantitatively. These methods yield remarkable accuracy and are proven to be sufficiently robust.

Keywords: *calibration-free laser-induced breakdown spectroscopy, new age coins, principal component analysis, partial least squares regression.*

ИССЛЕДОВАНИЕ СОВРЕМЕННЫХ МОНЕТ С ПОМОЩЬЮ ЛАЗЕРНОЙ АТОМНО-ЭМИССИОННОЙ СПЕКТРОСКОПИИ БЕЗ КАЛИБРОВКИ И ХЕМОМЕТРИЧЕСКИХ ПОДХОДОВ

S. Awasthi [1], R. Kumar [2*], R. K. Pandey [3], A. Kumar Rai [4*]

УДК 543.423:671.41

[1] Колледж М. М. Махила Университета V. K. S., Ара, Индия
[2] Университет Аллахабада, Прайградж, Индия; e-mail: rohit.02dec@gmail.com
[3] Университет нефти и энергетики Energy Acres, Бидхоли, Дехрадун, Индия
[4] Аллахабадский университет, Прайградж, Индия; e-mail: awadheshkrai@rediffmail.com

(Поступила 15 марта 2021)

Элементный состав монет достоинством в одну и две рупии, выпущенных в разные годы Резервным банком Индии (RBI), исследован с помощью лазерной атомно-эмиссионной спектроскопии (LIBS). С помощью LIBS можно выполнять анализ скрытых отпечатков пальцев образцов в режиме реального времени. Отмечены определенные различия в элементном составе монет, которые не упоминаются RBI. Результаты могут быть использованы в качестве справочного документа для выявления и предотвращения обращения поддельных монет. Концентрации компонентов, присутствующих в монетах, определены методом LIBS без калибровки. Статистические методы – анализ главных компонент и частичная регрессия наименьших квадратов – использованы для интерпрета-

**Full text is published in JAS V. 89, No. 4 (http://springer.com/journal/10812) and in electronic version of ZhPS V. 89, No. 4 (http://www.elibrary.ru/title_about.asp?id=7318; sales@elibrary.ru).

ции сложных данных, полученных в результате экспериментов LIBS. Методы имеют высокую точность и надежность.

Ключевые слова: *лазерная атомно-эмиссионная спектроскопия без калибровки, монеты нового века, анализ главных компонент, частичная регрессия наименьших квадратов.*

Introduction. The currency of any country is an important part of the economy and plays a very imperative role in its development. From ancient times, coins of a particular era have played a significant role in representing the circumstances of a country in that era. A piece of metal or other material bearing a distinctive marking to authorize its use as money is known as a coin. The coins of any country are mirrors of the culture, economy, and development of that country in that period, providing fruitful information on various topics, including life, politics, and the environment of the nation. Depending upon different aspects of a country, different coins are issued from time to time. The issuing authority of coins releases the form and structure of coins with different elemental compositions and mints. From ancient times to the modern era, coins of varying metal compositions are available in all parts of the world. The study of coins and related objects is called numismatics. Various researchers and numismatists are directly involved in coin collection and its study [1–5].

The study of old coins in India started long ago. The Indian Institute of Research in Numismatic Studies, situated in Nasik, Maharashtra, was established in 1980 to do this job. For a long time, the primary technique related to the compositional analysis of a coin has been the specific gravity method, by which only coins based on binary alloys could be analyzed. Nowadays, in India, coins are generally fabricated using materials like Fe, Cu, Mn, Cr, Al, Ag, Ni, etc. Various techniques, like particle-induced X-ray emission (PIXE), inductively coupled plasma mass spectrometry (ICP-MS), neutron activation analysis (NAA), atomic absorption spectrometry (AAS), energy dispersive X-ray fluorescence (EDXRF), etc., are available for elemental analysis of coins [6–10]. Apart from these techniques, LIBS is of particular interest because of its minimal-destructive, fast and sensitive nature, and also because it can do multi-elemental analysis at the same time. Also, LIBS is economical and requires less effort to run the setup. Lots of work has been done for elemental analysis using LIBS [11–13]. Here, LIBS was used to analyze a few coins (one- and two-rupee Indian coins of different years) to show how this technique can be routinely used for numismatic studies.

For quantitative analysis of samples in LIBS, generally two methods are used: the calibration curve method and the calibration-free LIBS (CF-LIBS) method. For the calibration curve method, standard or reference material that has a similar matrix as the unknown sample is required. However, if the reference materials of known concentrations of the same matrix are not available, then the calibration-free LIBS method has to be used, which is a technique that has been used for quantitative analysis of any kind of samples for many years [14–16]. In the case of coins, as no reference samples are available, the CF-LIBS method was used to calculate the concentration of different elements available in coins. A detailed discussion of the CF-LIBS technique has been given in a [15].

The LIBS spectra contain elemental details of the sample in the form of thousands of data points that are collected in less than 1 s. It is often not easy to analyze such high-dimensional data where only a few dimensions contain valuable information, while the other dimensions are not essential to describe the significant properties of the data in many instances. When high-dimensional data is compressed or visualized, some useful information may be missed. Ideally, the aim is to have the dimensions in the data that contain the most information and to ignore the less relevant dimensions. Implementation of the chemometric approach or multivariate tools for data processing helps in the hyperspectral analysis of large LIBS datasets. The most comprehensive benefit of such techniques is that they make use of different properties of the LIBS spectra themselves. Principal component analysis (PCA) is one of the most widespread supervised techniques for data compression, classification, and visualization [17–20] and has been used with LIBS for several years. PCA is an algorithm that reduces the dimensionality of the data and retains meaningful information by taking linear combinations of original variables and converting them into a new set of variables known as principal components (PCs) that contain the most information.

Partial least squares regression (PLSR) is another technique used in multivariate analysis, mostly in cases where the number of independent variables is significantly bigger than the number of data points. It is based on the principle of least squares whose criterion is to minimize the sum of squared deviations of data points from the regression line. Using PLSR, a relation between predictors and responses is obtained, which is useful for the prediction of unknown data. PLSR minimizes the residuals of the calibration model so that the spectral information can be effectively utilized and the possibility of overfitting can be reduced. Multi-

variate analysis combined with LIBS has been extensively used by several groups because it is a simple tool for qualitative studies and also gives good throughput for quantitative studies [17–25]. In this manuscript, PCA and PLSR are applied to LIBS spectra of coins of different years to take advantage of various features such as data identification, discrimination, visualization, regression, and prediction. Thus, in this report, for the first time, different statistical tools have been used with LIBS to estimate the concentrations of different elements in coins of one and two rupees issued by the Reserve Bank of India (RBI) in different years to provide a comprehensive detail about the different constituents of the coins, which may help in avoiding the circulation of counterfeit coins.

Experimental. Pulsed Nd:YAG laser (continuum sure lite III-10) at 532 nm was used here as an excitation source to create the plasma on the surface of readily available coins. The laser energy (15 mJ) and pulse repetition rate (4 Hz) were optimized to get the best signal to background ratio. An energy meter (Genetec-e model UP19K-30 H-VM-DO) was used to measure laser pulse energy. Four modules of the Czerny–Turner (C–Z) spectrometer (Ocean Optics LIBS2000+having a fixed gate delay of 1.5 μs), consisting of CCD (charged coupled device) with 14,336 pixels were used to analyze the collected emission. The detailed experimental procedure with the corresponding parameters is discussed elsewhere [19]. During the experiment, the averaged spectra of 10 laser shots on the sample were recorded to enhance the signal-to-noise ratio, and 10 such spectra for each sample were recorded. The LIBS spectra of different coins are organized in a matrix form consisting of huge variables that represent the intensities of spectral emission lines. Statistical treatment was performed using the Unscrambler-X software (CAMO Software India Pvt. Ltd.), which was applied to the data matrix. A representation of the whole procedure is depicted in Fig. 1.

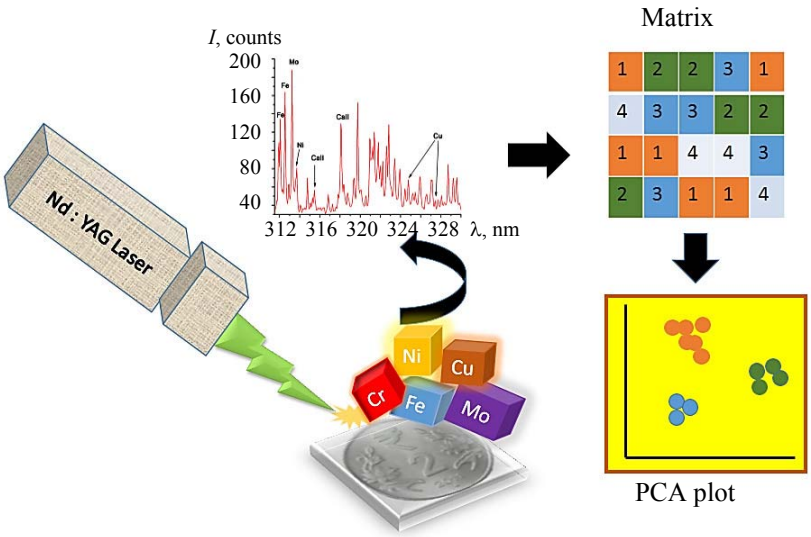

Fig. 1. Diagram showing the procedure of analysis.

Results and discussion. One-rupee coins were issued in 1996, 1998, 2001, 2002, 2004, 2009, 2010, 2011, and two-rupee coins were issued in 2006, 2007, 2008, 2009, 2010, 2011. According to the Reserve Bank of India (RBI), both one-and two-rupee coins are made up of ferritic stainless steel containing 83% Fe and 17% Cr. The LIBS spectra (Fig. 2) of these coins were recorded, and the spectral signatures of Fe and Cr were noted. Along with these spectral lines, the spectral lines of some minor elements like nickel, molybdenum, calcium, and copper were also observed. The NIST atomic spectroscopic database [26] and Chemical spectroscopy reference atomic data [27] were used to identify the various spectral lines present in the spectra. Figure 2 shows typical LIBS spectra of one-rupee coins from 1996 in the spectral ranges of 312–330 and 340–378 nm. Spectral signals of Fe, Cr, Ni, Ca, Cu, and Mo are observed in the LIBS spectrum of the coins. These spectral ranges were chosen because maximum emission lines were noted in them. Other emission lines, shown in Fig. 2, belong to the emission lines of the same elements present in the LIBS spectrum of coins.

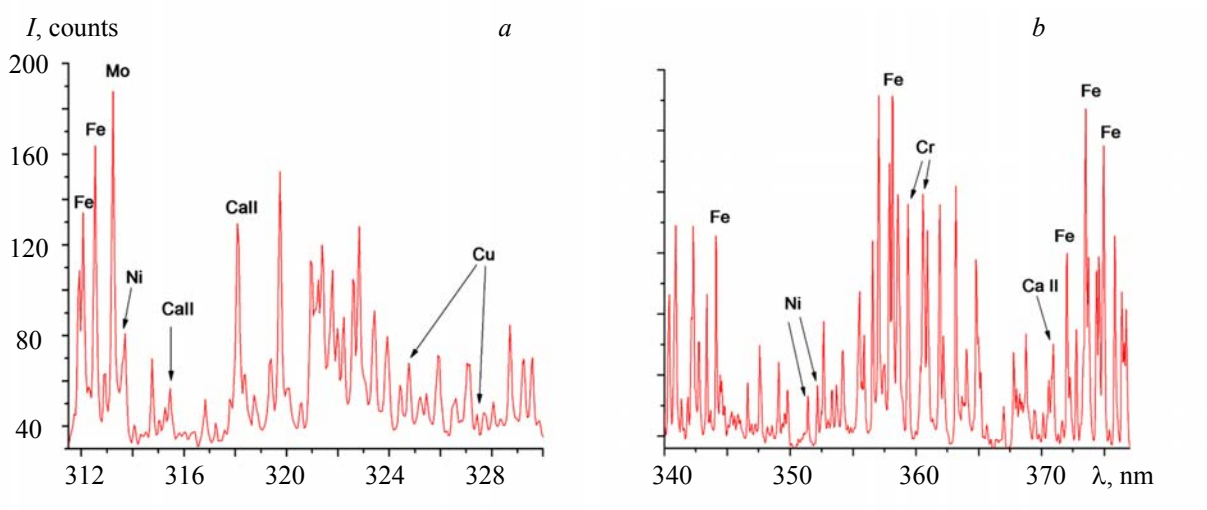

Fig. 2. LIBS spectra of a one-rupee Indian coin of the year 1996 in the spectral ranges 312–330 (a) and 340–378 nm (b).

Qualitative analysis of the spectrum shows that other elements (like Ca, Cu, Mo, and Ni) are present along with the matrix elements (Fe and Cr) of coins. It is possible that to make the coins more durable, these elements (Ca, Cu, Mo, and Ni) might have been added along with Fe, Cr. The presence of these elements in a coin may also occur during its manufacturing process. It is reported that Ni, Mo, and Cu are combined with the base metal to control corrosion in coins and various other artefacts [28]. These elements are coated on the surface of the metal to form a corrosion-resistant coating on the coin against the environment. Thus, it is assumed that these elements were added to coins for this reason. It is also reported that a small addition of Ca is used to improve machinability [29]. Elemental analysis of LIBS gives information about the composition of coins, which helps to identify unmarked or damaged coins that are otherwise difficult to identify. From this analysis, the difference between fake and original coins can be determined quickly and easily. Thus, our results show that this sort of analysis can be applied to any type of coin or archaeological artefact to determine various issues like attributions, chronology as well as the relationship between emissions produced in various eras, which could be an extension of this work.

Calculation of the concentrations of elemental species by the CF-LIBS method. The CF-LIBS method was proposed for quantitative measurement when appropriate reference standards are not available. The CF-LIBS method is used here for quantitative analysis of major as well as minor elements present in the samples. Before using this method, one has to ensure that the following conditions are satisfied by laser-induced plasma [16, 30, 31]: stoichiometric laser ablation, optically thin plasma, and local thermal equilibrium.

Stoichiometric ablation. The laser energy must be higher than the breakdown threshold of the material. It has been reported that if the laser irradiance is greater than 10^9 W/cm^2, the resulting plasma will be stoichiometric, since above this energy value, the base material arrives at its vaporization temperature, causing it to explode at the surface before the surface layer can vaporize [32]. For the present experiment, the calculated value of laser irradiance (laser energy per unit time per unit area) at 15 mJ of laser energy is 3.80×10^{12} W/cm^2, which is greater than 10^9 W/cm^2, thus verifying that the plasma is stoichiometric.

Optically thin plasma. Sometimes the emitted photons from the inner core of the plasma are absorbed within the plasma itself, thus in the resulting spectrum, the intensity of that particular photon is missing or self-absorbed phenomena are observed, which may lead to wrong information about elemental analysis. To check the optical thinness of the plasma, the spectral intensity ratio of two spectral lines having similar upper energy levels should be nearly equal to the ratio of their A_{ki}, g_k, and λ–1, i.e., for two spectral lines, the intensity ratio (I/I') should be nearly the same as $(A_{ki}g_kl')/(A'_{ki}g'_kl)$ [32, 33]. The measured intensity ratio of two Fe lines at 374.9 and 375.8 nm is 1.69 for a one-rupee coin of the year 1996. After calculating the $(A_{ki}g_kl')/(A'_{ki}g'_kl)$ for these two lines, it was found to equal 1.59. Thus, it can be seen that these ratios are nearly equal, which indicates that plasma is optically thin. This condition was checked for all coins in a similar fashion.

Local thermal equilibrium (LTE). For LTE, plasma should satisfy the necessary and sufficient conditions, which are stated in the following [31–34]. Necessary condition: The electron density of laser-induced

plasma must satisfy the McWhirter criteria. In other words, the experiment's electron number density must be greater than the lower limit defined by the following equation:

$$N_e > 1.6\times10^6\,[T]^{1/2}\,[\Delta E]^3, \tag{1}$$

where N_e is electron density, ΔE is the maximum energy difference between two states of an atom (eV), and T is plasma temperature (K).

Plasma temperature was calculated using the following Boltzmann relation:

$$\ln\frac{I_\lambda^{ki}}{A_{ki}\,g_k} = -\frac{E_k}{k_B T} + \ln\frac{C_s F}{U(T)}, \tag{2}$$

where I_λ^{ki} is the spectral intensity for wavelength λ; A_{ki} (cm^{-1}) is the transition probability; g_k is the statistical weight; E_k is the upper energy level; k_B is the Boltzmann constant; T is plasma temperature; F is the experimental factor; C_s is the concentration of a species of elements present in the sample, and $U(T)$ is the partition function.

The Boltzmann plot $\ln[I_\lambda^{ki}/(A_{ki}g_k)]$ vs E_k is plotted to determine the plasma temperature. Figure 3 shows the Boltzmann plot for a one-rupee coin in the year 1996. The plasma temperature is calculated from the slope of the plot and is found to be equal to 11241±819 K. By applying this value of plasma temperature, the electron density $N_e = 1.26\times10^{16}$ cm^{-3} was calculated using Eq. (1).

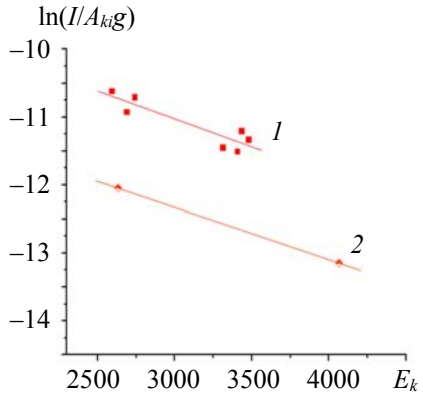

Fig. 3. Boltzmann plot for a one-rupee coin (1996) corresponding to different emission lines of elements: 1 – FeI, 2 – MoI

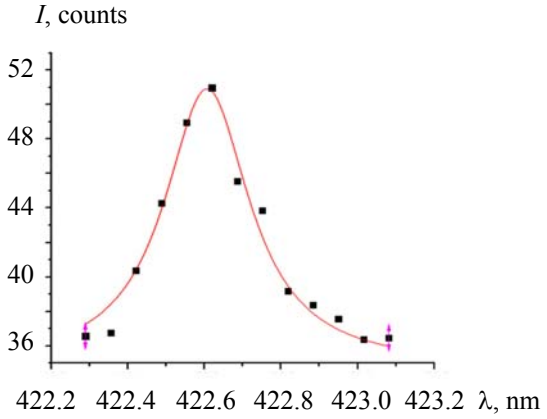

Fig. 4. Lorentzian plot of Ca (422.6 nm) for calculating the electron density by taking the FWHM of spectral line for a one-rupee coin (1996).

The electron density was calculated by measuring the FWHM (Δλ) of the Stark broadened line [34]. The expression is given by:

$$N_e = 10^{16}\Delta\lambda/2w. \tag{3}$$

Here, w is the electron impact parameter whose value is 9.25×10^{-4} nm for the Ca (422.6 nm) spectral line obtained from the [35], and Δλ is obtained using the relation $\Delta\lambda_{true} = (\Delta\lambda^2_{obs} - \Delta\lambda^2_{spectrom})^{1/2}$, where $\Delta\lambda_{true}$ is the FWHM of the Stark broadened line, $\Delta\lambda_{obs}$ is the measured line width, and $\Delta\lambda_{spectrom}$ is the instrumental width. In the present work, the electron density is calculated by measuring the FWHM of the spectral line of Ca at 422.6 nm for each coin. A Lorentzian plot of the atomic line of Ca (422.6 nm) present in the LIBS spectral of a one-rupee coin from 1996 is shown in Fig. 4. The measured value of electron density, calculated by Eq. (3) is found to be 8.22×10^{17} cm^{-3}, which is higher than the value of electron density (1.26×10^{16} cm^{-3}) for the McWhirter limit. The preceding result satisfies the necessary conditions for LTE.

Sufficient condition. Sufficient conditions hold when the ionization temperature is within 10% of the plasma temperature. The ionization temperature is calculated using the Saha–Boltzmann equation

$$\ln\frac{I_{mn}^{ion} A_{ki}^{atom} g_k^{atom}}{I_{ki}^{atom} A_{mn}^{ion} g_m^{ion}} = \ln\left(\frac{2(2\pi kTm_e)^{2/3}}{N_e h^3}\right) - \frac{E_{ion} - dE + E_m^{ion} - E_k^{atom}}{k_B T^{ion}}, \tag{4}$$

where I_{mn}^{ion} is the integrated emission intensity of the ionic line; I_{ki}^{atom} is the integrated emission intensity of the atomic line; m_e is electron mass; T is plasma temperature using the Boltzmann plot; h is the Planck's constant; T_{ion} is the ionization temperature; E_{ion} is the ionization potential of the atom; E_m and E_k are the upper energy levels of ionic and atomic species of the elements having transition probabilities A_{mn}^{ion} and A_{ki}^{atom} with statistical weights g_m^{ion} and g_k^{atom}, dE is the lowering of the ionization energy, and k is the Boltzmann constant.

Saha–Boltzmann's plot for Fe is plotted and is shown in Fig. 5. Using this plot, the ionization temperature was calculated, and its value was found to be equal to 12534±924 K, a value that is very close to the plasma temperature of 11241±819 K with 10% of the variation, which satisfies the sufficient condition for LTE. Thus, the necessary and sufficient conditions for LTE are satisfied. Similarly, LTE is verified for the laser-induced plasma of all other coins of different years.

Since the preceding three conditions are satisfied for each sample, the intensity of spectral lines can be used to calculate the concentration of constituents present in the LIBS spectra of all coins. Consequently, the following steps are used:

i) Initially, the area under the curve of spectral lines of elements is calculated.
ii) Plasma temperature is calculated using the Boltzmann plot.
iii) The intercept of the Boltzmann plot for each species is measured.
iv) The partition function for each species is calculated, which is defined as $U(T) = \sum g_k \exp(-E_k/k_B T)$.
v) Experimental parameter F is calculated.

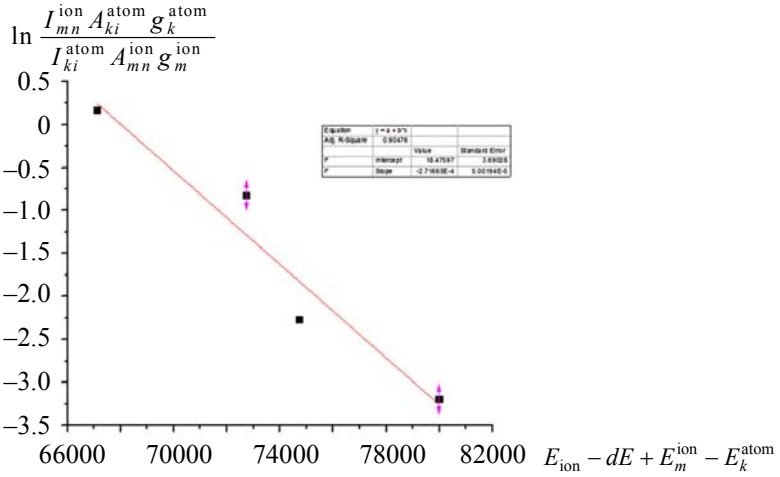

Fig. 5. Saha–Boltzmann plot of Fe to calculate the ionization temperature.

For calculating the experimental parameter, a basic assumption which says that the sum of concentrations of all species is equal to 100%, i.e., $\sum C_s = 1$ was used, which gives the value of the experimental parameter F.

The percentage concentration of elements calculated by the CF-LIBS method and present in the laser-induced plasma of one- and two-rupee coins of different years are tabulated in Table 1, as are the concentrations of various other elements. From this, it can be said that both one- and two-rupee coins of different years are not only made up of Fe and Cr but also have a concentration of other elements present in the composition of these coins, which are not reported in the database of the RBI. Hence, our investigation shows that LIBS is an appropriate technique for analysis in the field of numismatics.

Statistical treatment. In LIBS, the large datasets and the complexity of samples have extensive computational requirements. While compiling the data from LIBS analysis, it is strongly recommended that the obtained data be preprocessed because it contains unwanted background signals and the acquired results are sensitive to data preprocessing for increasing the accuracy of resultant features. In order to avoid numerical instability, it is also necessary to ensure that data used are mean-centered.

TABLE 1. Elemental Concentration (wt%) of Different Elements of One- and Two-Rupee Indian Coins

Year	Cu	Ca	Cr	Fe	Mo	Ni
One-Rupee Coins						
1996	0.07±0.001	4.69±0.02	18.87±0.05	70.30±0.67	1.90±0.003	4.14±0.02
1998	0.072±0.001	4.48±0.01	19.23±0.05	70.37±0.67	1.93±0.004	3.89±0.02
2000	0.065±0.0003	4.61±0.02	19.17±0.05	70.34±0.67	1.91±0.004	3.89±0.02
2001	0.12±0.001	2.67±0.012	18.40±0.07	72.77±0.65	2.01±0.01	3.99±0.02
2002	0.24±0.001	3.68±0.01	17.91±0.01	71.72±0.75	2.11±0.002	4.31±0.02
2004	0.17±0.001	3.21±0.015	18.68±0.05	71.55±0.70	2.11±0.004	4.25±0.02
2009	0.20±0.001	3.63±0.01	18.47±0.054	71.38±0.74	2.04±0.003	4.26±0.02
2010	0.11±0.001	2.46±0.01	17.70±0.055	73.53±0.70	2.04±0.004	4.13±0.02
2011	0.20±0.001	3.01±0.01	17.49±0.05	73.41±0.67	1.95±0.006	3.91±0.02
Two-Rupee Coins						
2006	0.17±0.001	5.19±0.03	16.82±0.04	72.02±0.67	1.88±0.004	3.90±0.02
2007	0.18±0.001	6.27±0.048	15.95±0.037	72.07±0.71	1.79±0.003	3.71±0.02
2008	0.14±0.001	3.93±0.02	17.27±0.043	72.87±0.62	1.92±0.004	3.83±0.02
2009	0.14±0.001	3.98±0.02	17.54±0.04	72.46±0.63	1.93±0.006	3.92±0.02
2010	0.18±0.001	4.73±0.02	18.14±0.05	70.88±0.65	1.97±0.01	4.07±0.02
2011	0.17±0.001	3.95±0.02	20.23±0.05	69.63±0.77	2.14±0.01	3.85±0.02

Principal component analysis. For the description of data, PCA was applied to the LIBS data of coins. A key idea behind PCA is to use orthogonal projections of data points as a way to compress data while minimizing the loss of information. In PCA, first, the mean is subtracted from the data and then it is divided by the standard deviation. After that, the eigenvalues and eigenvectors of the data covariance matrix are computed. Afterward, any data point can be projected onto the principal subspace spanned by the eigenvectors corresponding to the largest eigenvalues. The final result of a LIBS-based experiment consists of a multidimensional array of two spatial dimensions (x and y), which represent the map coordinates, along with one spectral dimension (λ). Each cell in this array represents the intensity of an emission line that belongs to a particular spectrum. The score image is generated after unfolding the results of the PCA applied to the X matrix (x^*y, λ).

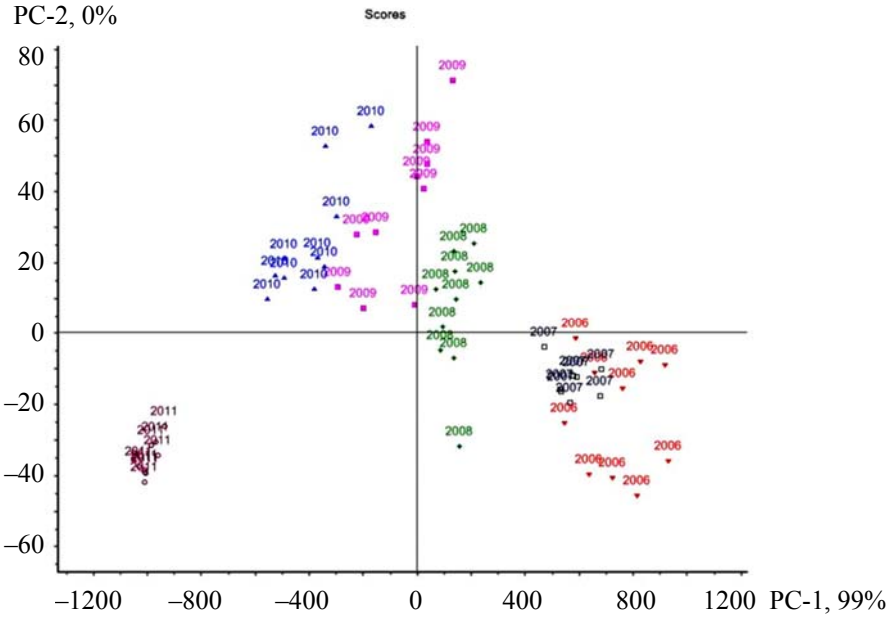

Fig. 6. PCA score plot for Indian two-rupee coins with variance of 99% at the PC1 axis and 0% along the PC2 axis.

For this purpose, data matrices 90×5589 and 60×5589 were prepared for one rupee and two-rupee coins, respectively. Figure 6 represents the 2D Score Plot of PCA for two-rupee coins. The score plot of PCA classifies the data of coins that have almost similar major and minor constituents. Here, ten spectra of each coin have been taken. In the data matrix, the total variance of 99.9% is explained by PC1 and PC2, which shows that the objects within each group are highly correlated. This result also shows that higher-order PCs are not needed because only the first two components of the principal component are sufficient to describe the data fully, while no relevant information about clustering is obtained from the other PCs. From Fig. 6, it is clear that these coins are divided into different groups on the basis of years. Similarly, the score plot for a one-rupee Indian coin is also drawn. From Fig. 6, it can be said that the concentrations of coins of different years are not the same, and thus they are divided into different groups. This figure also shows that although there is a slight difference between the concentrations of these coins, PCA has the capability of precise clustering. Thus, the PCA of LIBS data can provide a reliable and quick classification of coins.

Partial least square regression. Using PLSR, an attempt was made to develop a regression model, a relation between predictors (intensity) and responses (concentration of an element). The main aim of PLSR is to determine orthogonal latent variables that best explain the set of observed variables while predicting the output variables simultaneously. The accuracy of the model is assessed by the choice of an appropriate number of latent variables to describe the data. In reality, if a small number of components is chosen, then there is a possibility of not explaining all the relevant variance; on the other hand, if too many of them are selected, the model can overfit, i.e., the model cannot perform precisely for unknown variables. Upon noting such types of problems, cross-validation is used to estimate the accuracy of the performance in the predictive model, which is a good way to check the quality of the regression model.

Different sets of regression models have been prepared for the Fe and Cr elements present in one- and two-rupee coins. For predictors, the wavelength range corresponding to the particular element was selected, and in response, the concentration of that element was used to prepare the regression model. Of the ten replicate spectra for each sample, five spectra were selected for the training set and the rest of them as a test set. In this regard, a training matrix 30×150 was prepared, where 30 is the number of samples (five spectra of all six coins of rupee 2, and 100 are the intensity values for the spectral range 357–361 and 425–429 nm, which includes the wavelengths of Cr 357.8, 359.3, 360.5, 425.4, 427.4, and 428.9 nm. A typical regression model for the Cr of rupee 2 is shown in Fig. 7. The cross-validation method was used to test the robustness of the regression model. The data points in blue are the data points used to prepare the model, and the red ones are data for validation. R-square and root mean square error (RMSE) are two parameters to judge the model. For a good model, R-square should approach one, and RMSE should be close to zero. Once the values of R-square and RMSE are estimated based on training samples, the model can be used to predict the responses of any set of new samples. It is clear from Fig. 7 that the values of R-square for both Cr and Fe is 0.96, which is nearly one, and the value of RMSEC (0.05) is approaching zero, which reveals that the predictions and references are strongly correlated. In this way, the model is suitable for prediction.

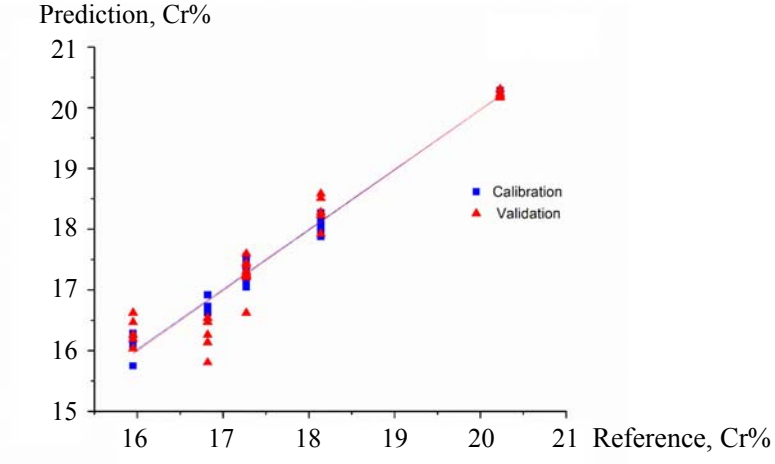

Fig. 7. Regression models (predicted vs. reference plots) for the concentration of Cr for two-rupee coins.

TABLE 2. Comparison of Elemental Concentration (wt.%) of Fe and Cr in Two- and One-Rupee Coins with CF-LIBS and PLSR

Year	Fe		Cr	
	CF-LIBS	PLSR	CF-LIBS	PLSR
Coin 2				
2006	72.02±0.67	72.01±0.11	16.82±0.04	16.22±0.36
2007	72.07±0.71	72.09±0.08	15.95±0.03	16.31±0.26
2008	72.87±0.62	72.09±0.08	17.27±0.04	17.52±0.06
2009	72.46±0.63	72.82±0.14	17.54±0.04	17.34±0.11
2010	70.88±0.65	70.90±0.22	18.14±0.05	18.33±0.21
2011	69.63±0.77	69.64±0.03	20.23±0.05	19.94±0.01
Coin 1				
1996	70.30±0.67	70.26±0.13	18.87±0.05	18.94±0.18
1998	70.37 ±0.67	70.42±0.18	19.23±0.05	19.28±0.16
2000	70.34±0.67	70.39±0.15	19.17±0.05	19.00±0.06
2001	72.77±0.65	72.81±0.14	18.40±0.07	18.37±0.14
2002	71.72±0.75	71.77±0.25	17.91±0.016	17.98±0.12
2004	71.55±0.70	71.51±0.14	18.68±0.05	18.67±0.06
2009	71.38±0.74	71.37±0.13	18.47±0.05	18.31±0.15
2010	73.53±0.70	73.58±0.04	17.70±0.05	17.71±0.30
2011	73.41±0.67	73.26±0.13	17.49±0.05	17.72±0.16

Concentrations of Fe and Cr are predicted for an unknown dataset using the PLSR model. Table 2 shows the predicted concentrations of Fe and Cr elements with standard deviation. From this table, it is clear that the predicted concentration is very close to the values determined by the CF-LIBS method. Thus, the concentrations of unknown coins can be predicted extensively using the model. Consequently, it can be demonstrated that multivariate analysis combined with LIBS is important for complete analysis and also to better understand complex data in a better manner.

Conclusions. The ability of LIBS, coupled with multivariate methods, as a rapid technique for analysis of new age coins is addressed. The analysis of one- and two-rupee Indian coins of different years using the LIBS technique shows that the spectral lines of major as well as minor elements that are not available in the Reserve Bank of India database are present in the LIBS spectra of these coins, which is helpful in the identification of counterfeit coins. It is noteworthy that there is no previous study available regarding compositional analyses of these coins, which may provide new data for numismatics research. Here it also proves that principal component analysis can perform discrimination of a variety of samples, no matter how minute the differences are.

REFERENCES

1. Srinivasan Chinnammai, *Economics and Finance*, **4**, No. 1 (2013).
2. Rajive Kumar, Anita Rani, Ram Mehar Singh, *J. Int. Sci. Technol*., **2**, No. 1, 1–4 (2014).
3. M. Fayze-Hassan, W. A. Ghaly, H. T. Mohsen, *Proc. 8th Conf. Nuclear and Particle Physics*, 183–189 (2011).
4. M. Hajivaliei, F. K. Nadooshan, *Nucl. Instr. Meth. B*, **289**, 56–58 (2012).
5. P. K. Nayak, T. R. Rautray, V. Vijayan, *Ind. J. Pure Appl. Phys.*, **42**, 319–322 (2004).
6. A. C. Mandal, *J. Phys. Sci.*, **19**, 103–107 (2014).
7. C. Andalo, M. Bicchieri, P. Bocchini, G. Casu, G. C. Galetti, P. A. Mando, M. Nardone, A. Sodo, M. P. Zappala, *Anal. Chim. Acta*, **429**, 279–286 (2001).
8. T. Cechak, J. Gerndt, M. Kubelik, L. Musilek, M. Pavlik, *Appl. Radiat. Isot*., **53**, No. 4-5, 565–570 (2000).
9. Y. Haruyama, M. Saito, T. Muneda, M. Mitai, R. Yamamoto, K. Yoshida., *Int. J. PIXE*, **9**, No. 3-4, 181–188 (1999).
10. B. B. Tripathy, T. R. Rautray, R. Satya Das, R. Manas Das, V. Vijayan, *Int. J. PIXE*, **19**, No. 3-4, 167–173 (2009).

11. S. Awasthi, R. Kumar, A. K. Rai, *J. Appl. Spectr.*, **84**, No. 5, 811–815 (2017).
12. Ashok Kumar Pathak, Rohit Kumar, Vivek Kumar Singh, Rahul Agrawal, Shikha Rai, Awadhesh Kumar Rai, *Appl. Spectrosc. Rev.*, **47**, No. 1, 14–40 (2012).
13. R. Kumar, A. Devanathan, N. L. Mishra, A. K. Rai, *J. Appl. Spectr.*, **86**, 942–947 (2019).
14. J. A. Aguilera, C. Aragón, G. Cristoforetti, E. Tognoni, *Spectrochim. Acta B*, **64**, 685–689 (2009).
15. A. Ciucci, M. Corsi, V. Palleschi, S. Rastelli, A. Salvetti, E. Tognoni, *Appl. Spectrosc.*, **53**, No. 8, 960–964 (1999).
16. Rohit Kumar, Awadhesh K. Rai, Devanathan Alamelu, Suresh K. Aggarwal, *Environ. Monitor. Assess*, **185**, 171–180 (2013).
17. V. C. Costa, S. dos Santos Ferreira, L. N. Santos, M. A. Sperança, C. Santos da Silva, G. A. Sodré, E. R. Pereira-Filho, *J. Appl. Spectr.*, **87**, 378–386 (2020).
18. Spizzichino Valeria, Fantoni Roberta, *Spectrochim. Acta B*, **99**, 201–209 (2014).
19. Shikha Awasthi, Rohit Kumar, G. K. Rai, A. K. Rai, *Opt. Laser Eng.*, **79**, 29–38 (2016).
20. Shanshan Qiu, Liping Gao, Jun Wang, *J. Food Eng.*, **144**, 77–85 (2015).
21. T. F. Boucher, M. V. Ozanne, M. L. Carmosino, M. Darby Dyar, S. Mahadevan, E. A. Breves, K. H. Lepore, S. M. Clegg, *Spectrochim. Acta B*, **107**, 1–10 (2015).
22. Manjeet Singh, Arnab Sarkar, *J. Appl. Spectr.*, **85**, 962–970 (2018).
23. G. S. Senesi, R. A. Romano, B. S. Marangoni, G. Nicolodelli, P. R. Villas-Boas, V. M. Benites, D. M. B. P. Milori, *J. Appl. Spectr.*, **84**, 923–928 (2017).
24. Shikha Awasthi, Rohit Kumar, Alamelu Devanathan, R. Acharya, A. K. Rai, *Anal. Chem. Res.*, **12**, 10–16 (2017).
25. Taoreed O. Owolabi, Mohammed A. Gondal, *Anal. Chim. Acta*, **1030**, 33–41 (2018).
26. National Institute of Standards and Technology, Electronic database; http://physics.nist.gov/PhysRefData/ASD/lines form.html.
27. W. R. Brode, *Chemical Spectroscopy*, Wiley, New York (1958).
28. H. R. Bakhsheshi-Rad, M. H. Idris, M. R. Abdul-Kadir, A. Ourdjini, M. Medraj, M. Daroonparvar, E. Hamzah, *Mater. Design*, **53**, 283–292 (2014).
29. H. Kankaanpää, H. Pöntinen, A. S. Korhonen, *Mater. Sci. Technol.*, **3**, No. 2, 155–158 (1987).
30. R. Agrawal et al., *Food Biophys.*, **6**, 527–533 (2011).
31. Gulab S. Maurya et al., *J. Nucl. Mater.*, **444**, 23–29 (2014).
32. J. P. Singh, S. N. Thakur, *Laser-Induced Breakdown Spectroscopy,* First ed., Elsevier (2007).
33. A. W. Mziolek, V. Palleschi, I. Schechter, *Laser-Induced Breakdown Spectroscopy (LIBS) Fundamentals and Applications*, Cambridge University Press, 122–170 (2006).
34. A. H. Galmed, M. A. Harith, *Appl. Phys. B, Laser and Opt.*, **91**, 651–660 (2008).
35. H. R. Griem, *Plasma Spectroscopy*, McGraw-Hill, New York (1964).